Res Chem Intermed
DOI 10.1007/s11164-016-2448-4

Synthesis of sulfonated carbon-based solid acid as a novel and efficient nanocatalyst for the preparation of highly functionalized piperidines and acylals: a DFT study

Zahra Hoseinabadi[1] · Seied Ali Pourmousavi[1,2] · Mahdi Zamani[1]

Received: 16 October 2015 / Accepted: 16 January 2016

Abstract A novel carbon-based solid-acid nanocatalyst (Sta-SO_3H) was simply prepared for the first time by the thermal treatment of sulfuric acid with starch at 180 °C in a sealed autoclave. The catalytic activities of Sta-SO_3H as an efficient and reusable catalyst were investigated by the condensation reaction of aldehyde, amine and β-keto ester for the synthesis of functionalized piperidines under solvent-free conditions at room temperature in good to high yields. Density functional theory calculations were used to study the structure of methyl 1,2,6-triphenyl-4-(phenylamino)-1,2,5,6-tetrahydropyridine-3-carboxylate (MPPC) as well as the thermochemistry of the multicomponent reaction. The theoretically calculated infrared and ^1H nuclear magnetic resonance spectra of MPPC were compared to the experimental data. It was found that the synthesis of MPPC is exothermic accompanied by a decrease in entropy, internal energy and Gibbs free energy of reaction. Good consistency between the calculated and observed spectral data was found. Also, Sta-SO_3H has been developed for the synthesis of acylals (1,1-diacetate) in high yields through the reaction of aldehydes with acetic anhydride at room temperature under solvent-free conditions. The mild conditions, eco-friendliness, excellent yields, short reaction times and use of an inexpensive and reusable catalyst are important features of this method.

✉ Seied Ali Pourmousavi
pourmousavi@du.ac.ir

[1] School of Chemistry, Damghan University, 36716-41167 Damghan, Iran

[2] Institute of Biological Sciences, Damghan University, 36716-41167 Damghan, Iran

Published online: 02 February 2016

Graphical Abstract

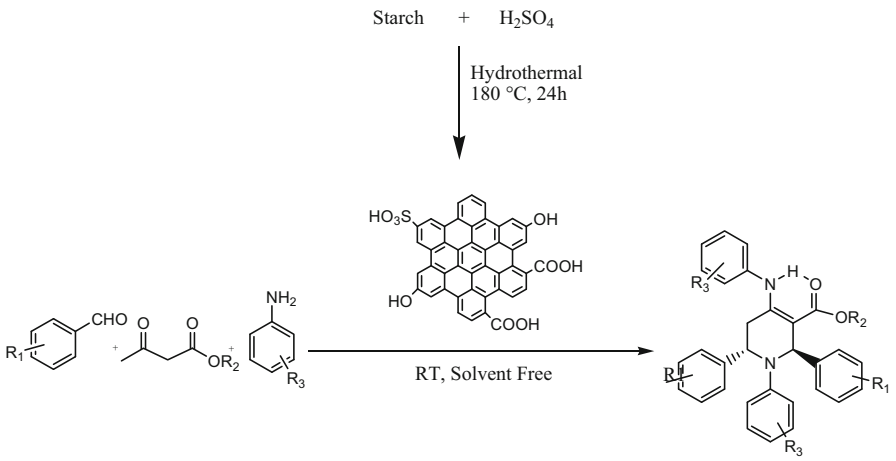

Keywords Multicomponent reaction · DFT · Thermochemistry · Piperidine · 1,1-Diacetates

Introduction

The principles of green chemistry and increasing concerns about environmental issues have stimulated the research for recyclable strong solid acids to replace conventional toxic and corrosive acid catalysts, such as sulfuric acid [1]. Solid acid catalysts have received much attention for the potential substitution of the homogeneous acids with the advantages of easy separation and reusability [2]. Carbon-based catalysts have several advantages as solid catalysts because of the unique properties of carbon possessing sp, sp^2 and sp^3 bondings resulting in the ability to make different structures, such as layers, tubes and spheres. Carbon can be easily functionalized in amorphous to crystalline structures especially in the amorphous form [3–8]. Sulfonated (SO_3H-bearing) carbon materials have been reported to act as strong solid-acid catalysts. Hara's group first prepared sulfonated carbon catalysts via the sulfonation and carbonization of polycyclic aromatic hydrocarbons [9]. Recently, Hara et al. prepared a series of acidic carbon catalysts through the direct carbonization of raw materials such as sugar and cellulose followed by the sulfonation of the resulting carbons, and found that such acidic carbon materials exhibited good catalytic behavior [10]. The solid acid catalysts were generally prepared through two steps. In the first step, the carbonization of biomass was carried out to form polycyclic aromatic carbon sheets. Then, the aromatic carbon sheets were sulfonated to introduce the sulfonic acid groups. The carbonization process was taken at high temperature for a long period and large amount of wastes were produced during the process, which resulted in serious pollution. Efficient procedures for the synthesis of carbon-based solid acid through one-step hydrothermal carbonization have been developed [11].

Reactions whereby three or more different components are combined in one reaction vessel, leading to the formation of a single product, are summarized under the term multicomponent reactions (MCRs) [12–15]. Recently, MCRs have emerged as a powerful synthetic tool in organic synthesis due to their advantages over conventional multi-step synthesis. In addition, MCRs are eco-friendly and have superior atom economy, as well as avoiding costly purification processes and protection–deprotection steps with minimum synthetic effort and time [16–20].

The piperidines and their analogues are important heterocycles that are present in many naturally occurring alkaloids, biologically active synthetic molecules, and organic fine chemicals [21–23]. Thus, the synthesis of highly substituted piperidines has gained considerable attention, and a number of procedures have been developed using several approaches [17, 24–36]. In recent times, very few methods have been reported describing the one-pot multicomponent synthesis of functionalized piperidines, based on catalysts such as L-proline/TFA [37], bromodimethylsulfonium bromide (BDMS) [17], tetrabutylammonium tribromide (TBATB) [19], molecular iodine [16], $InCl_3$ [36], CAN [38], $ZrOCl_2{\cdot}8H_2O$ [39], picric acid [40], $[K^+PEG]Br_3^-$ [41], $Bi(NO_3)_3{\cdot}3H_2O$ [18], VCl_3 [42], BF_3. SiO_2 [43], AcOH [44], Fe@Si–Gu–Prs [45], SSA [46] and tartaric acid [20]. However, some of these procedures suffer from the drawbacks of multistep synthesis, long reaction times, reaction work-ups, highly toxic catalysts, being difficult to prepare, having harsh reaction conditions and expensive catalysts and procedures.

Here, we report for the first time a facile procedure for the synthesis of Sta-SO_3H through the heat treatment of sulfuric acid and starch. These catalysts showed good activity in the condensation reaction of aldehyde, amine and β-keto ester to produce piperidine derivatives and the synthesis of acylals. Then, density functional theory (DFT) calculations were used to study the structure of the general product as well as the thermochemistry of the multicomponent reaction.

Experimental

Materials and instruments

All chemicals were purchased from Merck. All the reagents and chemicals were obtained from Merck and used without further purification. The development of reactions were monitored by TLC on Merck pre-coated silica gel 60 F254 aluminum sheets, visualized by UV light. IR spectra were recorded on a Shimadzu FT-IR 8300 Spectrophotometer using the KBr pellets technique. The known products were identified by comparison of their melting points and spectral data with those reported in the literature. ^{1}H NMR spectra were recorded at ambient temperature on a BRUKER AVANCE DRX-400 MHz spectrophotometer using $CDCl_3$ as the solvent and TMS as an internal standard. XRD patterns were recorded by an X-ray diffractometer (Philips-PW1800). The morphologies of the catalyst were studied by a field emission scanning electron microscope (FESEM; Mira 3-XMU) with an accelerating voltage at 10 kV.

Catalyst preparation

The Sta-SO_3H was prepared via thermal treatment of the mixture of sulfuric acid/starch at 180 °C. In a typical synthesis, 2 g of starch and 10 mL of H_2SO_4 were combined in a 100-mL Teflon-sealed autoclave and maintained at 180 °C for 24 h. The obtained black products were filtered and washed with hot distilled water and then oven-dried at 80 °C overnight. As a comparison, 2 g of starch without adding H_2SO_4 was also treated in the similar way and was denoted as Sta-180.

General procedure for the synthesis of piperidines

Aromatic aldehyde (2 mmol), amine (2 mmol), β-keto ester (1 mmol) and 0.035 g of catalyst were eroded for 20 min at room temperature. The progress of the reaction was monitored by TLC. The thick precipitate was filtered off and washed with ethanol to give pure products. All products were characterized on the basis of FT-IR, ^{1}H-NMR and ^{13}C-NMR spectral data, and by comparing the spectra to those of authentic samples or reported data.

General procedure for preparation of 1,1-diacetates

To a mixture of aldehyde (1 mmol) and acetic anhydride (3 mmol), Sta-SO_3H (0.035 g) was added and the mixture was stirred at room temperature. The progress of the reaction was monitored by TLC. After disappearance of the starting material, CH_2Cl_2 (10 mL) was added and the mixture was filtered off. The catalyst was washed with CH_2Cl_2 and then the organic layer was washed with saturated $NaHCO_3$ (10 mL) and water two times (2 × 10 mL) and dried with anhydrous $MgSO_4$, filtered and the solvent was evaporated to give the pure desired compound.

Spectral data of some selected products

Methyl-2,6-bis(4-methylphenyl)-1-phenyl-4-phenylamino-1,2,5,6-tetrahydropyridine-3-carboxylate (Table 3, entry 1)

White solid; mp: 210–217 °C; IR (KBr): 1657, 1591 cm^{-1}; ^{1}H-NMR (400 MHz, $CDCl_3$) δ: 10.25 (1H, s, NH), 7.19 (2H, d, J = 8.0 Hz, ArH), 7.02 (11H, m, ArH), 6.59 (1H, t, J = 7.2 Hz, ArH), 6.52 (2H, d, J = 8.0 Hz, ArH), 6.39 (1H, s, H-2), 6.30 (2H, d, J = 8.0 Hz, ArH), 5.11 (1H, d, J = 3.2 Hz, H-6), 3.92 (3H, s, OMe), 2.86 (1H, dd, J = 15.2, 5.6 Hz, H-5′), 2.75 (1H, dd, J = 15.2, 2.4 Hz, H-5″), 2.33 (3H, s, Me), 2.32 (3H, s, Me); ^{13}C-NMR (100 MHz, $CDCl_3$) 168.8 (C=O), 156.5 (C-4), 147.2, 141.1, 139.8, 138.1, 136.8, 136.0, 129.4, 129.1, 129.0, 128.9, 126.7, 126.5, 126.0, 125.8, 116.1, 113.0, 98.2 (C-3), 58.1 (C-6), 55.0 (C-2), 51.2, 33.8 (C-5), 21.3, 21.2.

Methyl-1,2,6-triphenyl-4-phenylamino-1, 2, 5, 6-tetrahydropyridine-3-carboxylate (Table 3, entry 5)

White solid; mp: 195–196 °C; IR (KBr): 1663, 1591 cm^{-1}; ^{1}H-NMR (400 MHz, $CDCl_3$) δ: 10.27 (1H, s, NH), 7.24–7.32 (8H, m, ArH), 7.15 (2H, d, $J = 6.4$ Hz, ArH), 7.04–7.09 (5H, m, ArH), 6.67 (1H, t, $J = 7.3$ Hz, ArH), 6.49 (2H, d, $J = 8.2$ Hz, ArH), 6.43 (2H, d, $J = 7.6$ Hz, ArH), 6.38 (1H, s, H-2), 5.11–5.12 (1H, d, H-6), 3.93 (3H, s, OMe), 2.85 (1H, dd, $J = 15.0$, 5.8 Hz, H-5′), 2.77 (1H, dd, $J = 15.0$, 2.1 Hz, H-5″); ^{13}C-NMR (100 MHz, CDCl3) 168.7 (C=O), 156.4 (C-4), 147.1, 144.0, 142.9, 137.9, 129.0, 128.9, 128.8, 128.4, 127.3, 126.8, 126.5, 126.0, 125.9, 116.3, 113.0, 98.0 (C-3), 58.3 (C-6), 55.2 (C-2), 51.2, 33.8 (C-5).

Ethyl-2,6-bis(4-methylphenyl)-1-phenyl-4-phenylamino-1,2,5,6-tetrahydropyridine-3-carboxylate (Table 3, entry 6)

White solid; mp: 229–231 °C; IR (KBr): 1649, 1592 cm^{-1}; ^{1}H-NMR (400 MHz, $CDCl_3$) δ:10.33 (1H, s, NH), 7.28 (2H, d, $J = 8.0$ Hz, ArH), 7.13–7.08 (11H,m, ArH), 6.63 (1H, t, $J = 7.2$ Hz, ArH), 6.57 (2H, d, $J = 8.8$ Hz, ArH), 6.45(1H, s, H-2), 6.34 (2H, d, $J = 7.6$ Hz, ArH), 5.15 (1H, d, $J = 2.4$ Hz, H-6), 4.53–4.45 (1H, m, OCH_aH_b), 4.40–4.32 (1H, m, OCH_aH_b), 2.90 (1H, dd, $J = 15.2$, 5.6 Hz, H-5′), 2.8 (1H, dd, $J = 15.2$, 2.4 Hz, H-5″), 2.37 (3H, s, Me), 2.36 (3H, s, Me), 1.50 (3H, t, $J = 7.2$ Hz, OC–CH_3); ^{13}C-NMR (100 MHz,$CDCl_3$) 168.4 (C=O), 156.2 (C-4), 147.2, 141.2, 139.9, 138.2, 136.8, 135.9, 129.4, 129.1, 129.0, 128.9, 126.7, 126.5, 125.9, 125.7, 116.1, 113.1, 98.5 (C-3), 59.8, 58.1 (C-6), 55.0 (C-2), 33.8 (C-5), 21.3, 21.2, 15.0.

Ethyl-2,6-bis(4-chlorophenyl)-1-phenyl-4-phenylamino-1,2,5,6-tetrahydropyridine-3-carboxylate (Table 3, entry 7)

White solid; mp: 206–208 °C; IR (KBr): 1652, 1597 cm^{-1}; ^{1}H-NMR (400 MHz, $CDCl_3$) δ:10.32 (1H, s, NH), 7.21–7.25 (8H, m, ArH), 7.03–7.16 (5H, m, ArH), 6.67 (1H, t, $J = 6.8$ Hz, ArH), 6.49 (2H, d, $J = 8.2$ Hz, ArH), 6.44 (2H, d, $J = 7.3$ Hz, ArH), 6.35 (1H, s, H-2), 5.12 (1H, d, H-6), 4.44–4.52 (1H, m, OCH_aH_b), 4.31–4.39 (1H, m, OCH_aH_b), 2.86 (1H, dd, $J = 15.1$, 6.0 Hz, H-5′), 2.77 (1H, dd, $J = 15.1$, 2.4 Hz, H-5″), 1.48 (3H, t, $J = 7.3$ Hz, OC–CH_3); ^{13}C-NMR (100 MHz, $CDCl_3$) 168.4 (C=O), 156.2 (C-4), 146.6, 142.5, 141.0, 137.7, 133.0, 132.3, 129.2, 128.9, 128.6, 128.2, 127.9, 126.2, 125.9, 116.9, 113.1, 97.6 (C-3), 57.5 (C-6), 54.8 (C-2), 51.3, 33.8 (C-5).

Computational details

In this study, the recently developed M06-2X/6-311G(*d*,*p*) meta hybrid density functional which is one of the recommended DFT methods for applications involving main-group thermochemistry [47] was used for the structural, spectroscopic and the thermochemical analysis of MPPC. The vibrational frequencies were calculated to check the nature of the minimum structure, the prediction of IR

spectrum and the calculation of thermochemical data for the multicomponent reaction (Scheme 1).

The difference of the sum of electronic energy and thermal energy for the reactants and products was used for the calculation of the internal energy of the reaction ($\Delta_r U°$). The difference of the sum of electronic energy and thermal enthalpy for the reactants and products was used for the calculation of the standard enthalpy of the reaction ($\Delta_r H°$). The entropy of the reaction ($\Delta_r S°$) was evaluated on the basis of thermodynamic functions obtained by vibrational analysis results and the statistical thermodynamic method. The Gibbs free energy of reaction ($\Delta_r G°$) was calculated via Eq. (1), where T is 298.15 K.

$$\Delta_r G^\circ = \Delta_r H^\circ - T\Delta_r S^\circ \tag{1}$$

^{1}H NMR chemical shifts (δ, ppm) versus tetramethylsilane (TMS) were calculated by the gauge-independent atomic orbitals (GIAO) method [48, 49] using the more convenient B3LYP/6-311+G(2*d*,*p*) density function. All calculations were performed using the Gaussian 09 program package [50].

Results and discussion

Characterization of the novel catalyst

The Sta-SO_3H sample has a broad and very weak XRD pattern (shown in Fig. 1), confirming that the Sta-SO_3H is still amorphous and far from the graphitic carbon [51]. Two broad and diffuse peaks at 2 angles of 20–30° and 40–50° are due to the carbon (0 0 2) and (1 0 0) reflections, respectively. These diffraction patterns reflect that Sta-SO_3H is an amorphous carbon composed of aromatic carbon sheets oriented in a random fashion. Structurally, the carbon framework of Sta-SO_3H is approximately consistent with the others reported in the literatures [52, 53]. Nevertheless, the peaks of the 0 0 2 and 1 0 0 reflections are changed slightly in their position and shape. This may be due to the differences in carbonization mechanisms

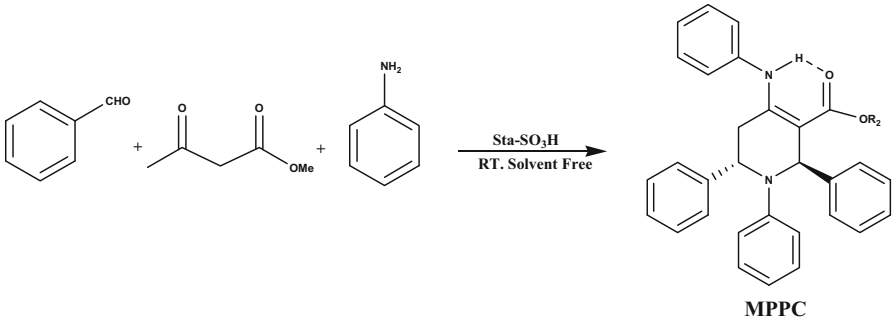

Scheme 1 Synthesis of MPPC

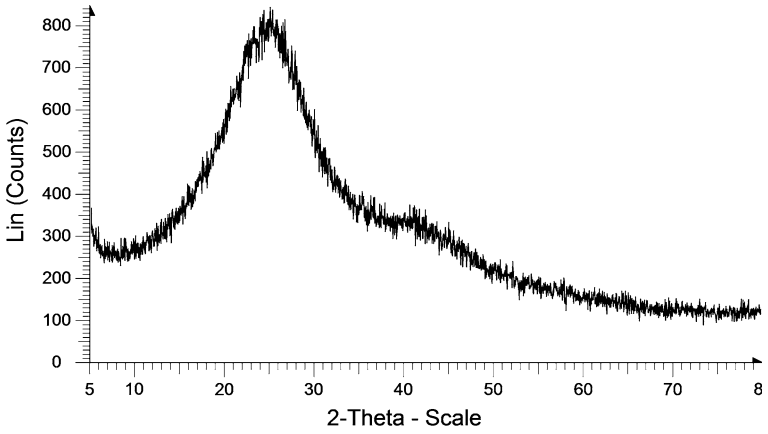

Fig. 1 The XRD patterns of the Sta-SO_3H

of starch and other carbohydrates, which impact the size and orientation degree of graphite crystallite.

The FT-IR spectra of Sta-180 and Sta-SO_3H are shown in Fig. 2. Compared to sample Sta-180, the distinguished features of Sta-180 were the presence of new absorption bands at 1032 cm^{-1}, 1007 cm^{-1} and 1118 cm^{-1}, which are attributed to SO_3H groups. This indicates that the SO_3H groups were successfully incorporated into the carbon framework by adding H_2SO_4 in the synthesis system. On the other hand, the bands due to –OH stretching at 3420 cm^{-1}, C=O stretching at 1710 cm^{-1}, C=C bonds stretching at 1620 cm^{-1}, and C–C bonds stretching at 1250 cm^{-1} were observed for both samples independent of the sulfonation.

Structural analyses of catalyst were carried out using FESEM, and representative images are illustrated in Fig. 3. Sta-SO_3H was found to be composed of nonspherical and irregular grains of < 20 nm in size. The sample was gold-coated before scanning.

The acidity of the novel carbon-based solid acid was 8 mmol/g, which were determined by acid–base back titration. The elemental analysis gave the results: C 61.79 %; H 1.634 %; S 1.6 %. The results indicated that the almost all the element S existed in the catalyst in the form of sulfonic groups.

If all the sulfur element in the catalysts was assumed to be $–SO_3H$ groups, the acid site densities of the catalysts were 0.5–2 mmol H^+/g depending on the synthesis conditions. But the acid titration experiments demonstrated much higher acid site densities than the estimations based on sulfur elemental analysis. The reason is that abundant phenolic –OH and –COOH groups were generated in the process of partial oxidation by concentrated sulfuric acid. The strong sulfonation agent may also oxidize aliphatic CH_3/CH_2 groups to carboxylic acid groups which may further explain the significant increase in total acid density after sulfonation. According to the reported carbon-based solid acid, the proposed carbon structure is schematically illustrated in Scheme 2 [54].

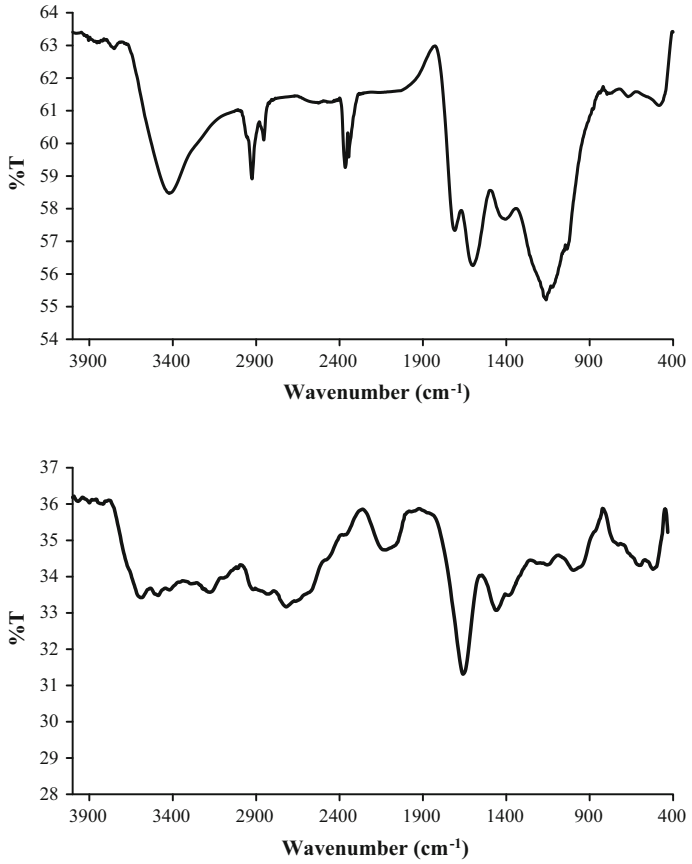

Fig. 2 The IR spectra of the Sta-SO_3H (*top*) and the Sta-180 (*bottom*)

Catalytic procedure for the synthesis of piperidines

Characterizations showed that the acid site densities of the catalyst were 8 mmol H^+/g and, in continuation of our work in the application of heterogeneous catalyst [55–58], the catalytic performances were also investigated in the synthesis of highly substituted piperidines as multicomponent reactions (Scheme 3).

A series of trial reactions were performed with a combination of 4-methylbenzaldehyde, aniline, and methyl acetoacetate to obtain reaction conditions. Several solvents were screened prior to concluding that reactions carry out without any solvent (Table 1).

Thus, the optimum conditions for synthesis of highly substituted piperidines was achieved by treatment of 1 mmol of aldehyde, 2 mmol aniline and 1 mmol β-ketoester in the presence of Sta-SO_3H (0.35 g) at room temperature under solvent-free conditions. Therefore, we employed the above conditions for the conversion of various aldehydes and amines to the highly substituted piperidines under solvent-

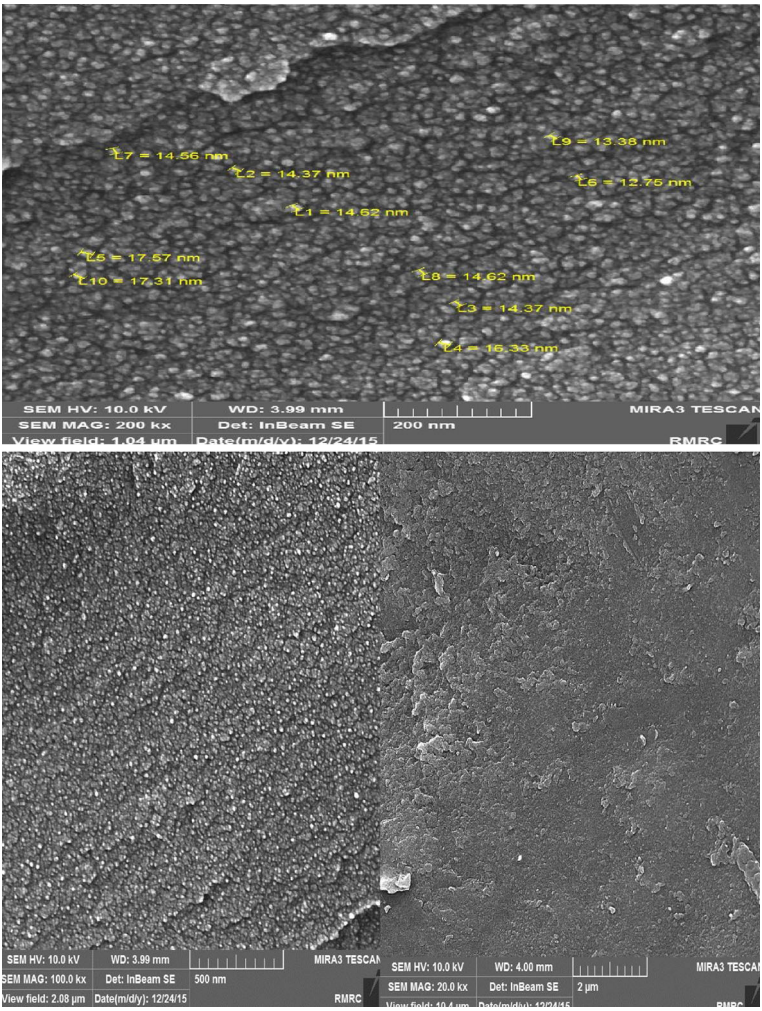

Fig. 3 The SEM image of Sta-SO_3H

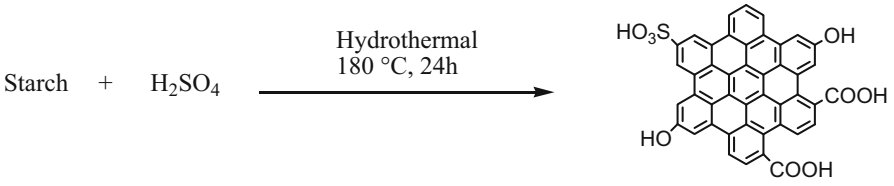

Scheme 2 Synthesis of Sta-SO_3H and proposed structure for the catalyst

free conditions (Table 2). The structures of all the compounds were characterized by a comparison of their IR and NMR spectra with authentic samples. Also, the relative stereochemistry of these piperidines has been confirmed by single X-ray

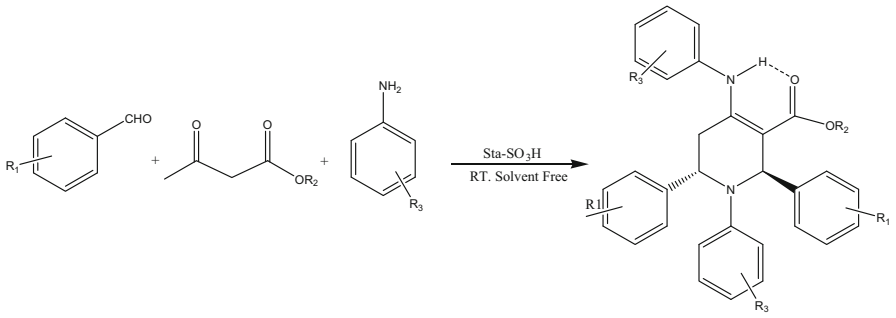

Scheme 3 Synthesis of functionalized piperidines

Table 1 Optimization of the reaction conditions for the synthesis of functionalized piperidine[a]

Entry	Solvent	Catalyst (g)	Time	Yield (%)
1	CH_3OH	0.035	5 h	63
2	ETOH	0.035	5 h	61
3	Ethyl acetate	0.035	5 h	61
4	CH_2Cl_2	0.035	5 h	62
5	*n*-Hexane	0.035	5 h	61
6	Neat	Neat	20 min	28
7	Neat	0.0175	30 min	48
8	Neat	0.035	20 min	67
9	Neat	0.07	20 min	67

[a] Conditions: 4-methylbenzaldehyde (2 mmol), aniline (2 mmol), and methyl acetoacetate (1 mmol) and Sta-SO_3H (0.035 g) at RT under solvent-free conditions

crystallography analysis in previously reported literature [16–19, 38, 39, 43, 59–61], and the relative stereochemistry of the products in the present work was proved by comparison of spectroscopic data of some products with those authentic samples.

Using the optimal reaction conditions, the reaction of benzaldehyde with aniline and methyl acetoacetate was studied and the product was obtained in good yield (Table 2, entry 5). The reactions of various aromatic aldehydes containing substituents in the aromatic ring such as OMe, Cl, Br, and NO_2 with aniline and methyl acetoacetate were performed under the same reaction conditions. The reaction time and the percentage yield of the products are shown in Table 2. However, in the case of 3- and 4-nitrobenzaldehydes the products were obtained in low yield (Table 2, entries 4 and 8). This may be attributed to the formation of more stable imine having an extra conjugation in the presence of nitro group. This stable imine is less reactive.

Various anilines with substituents such as Me, OMe, Br, and NO_2 were treated with 4-methylbenzaldehyde and methyl acetoacetate under identical reaction conditions. All these reactions underwent smoothly to provide the corresponding piperidine derivatives, in moderate to good yields (Table 2, entries 8–14).

The reaction was further examined with ethyl acetoacetate as a 1, 3-dicarbonyl compound and the desired piperidine derivative was obtained in good yields

Table 2 Synthesis of functionalized piperidines using Sta-SO_3H

Entry	Substrate	Product[a]	Time (min)	Yield[b] (%)	m.p. (°C) [Ref.]	
					Found	Reported
1	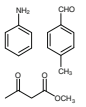	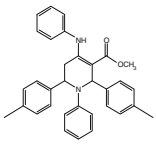	20	67	210–217	215–217 [16]
2	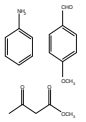	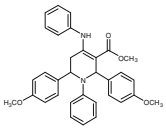	20	68	180–182	181 [62]
3	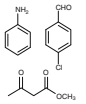	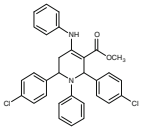	20	71	223–225	223–225 [42]
4	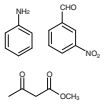	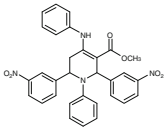	40	47	181–183	182 [62]
5	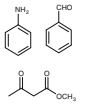	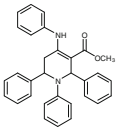	50	62	195–196	195–196 [42]
6	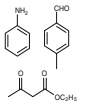	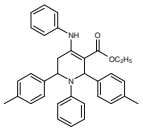	50	65	229–231	228–231 [16]
7	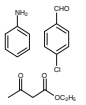	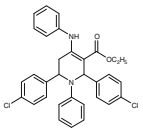	50	73	206–208	206–208 [42]
8	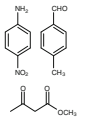	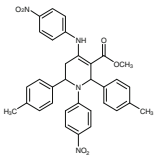	40	Trace	252–255	253–255 [16]
9	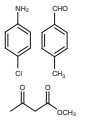	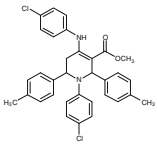	50	55	180–181	181–183 [42]

Table 2 continued

Entry	Substrate	Product[a]	Time (min)	Yield[b] (%)	m.p. (°C) [Ref.]	
					Found	Reported
10	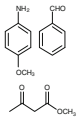	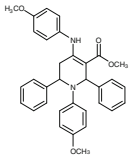	40	66	223–225	–
11	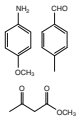	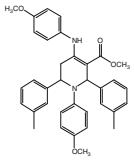	45	67	225–227	223–225 [42]
12	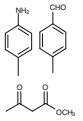	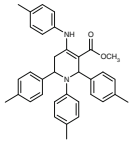	45	65	206–208	205–207 [42]
13	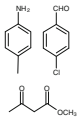	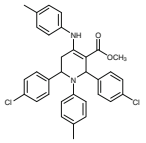	40	69	213–215	213–215 [62]
14	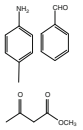	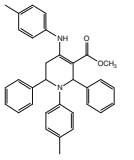	40	66	223–225	220–222 [62]

Conditions: aldehyde (2 mmol), amine (2 mmol), methyl acetoacetate (1 mmol), Sta-SO3H (0.035 g), at roomtemperature under solvent free conditions

[a] All compounds were characterized by 1H-NMR, 13C-NMR, IR

[b] Isolated yield

(Table 2, entries 7 and 8). This confirms that the alkoxy (–OR) moiety present in the ester functionality does not have any major role in determining the course of the reaction.

In order to show the merit of the present work in comparison with recently reported protocols, we compared the results of condensation of 4-chlorobenzaldehyde, aniline and methyl acetoacetate in the presence of various catalysts (Table 3). The results show that Sta-SO_3H promotes the reactions effectively as far the amount of catalyst and reaction times are concerned.

The reusability of the catalyst is of great importance for commercial feasibility; therefore, the recovery and reusability of Sta-SO_3H was investigated in the reaction of 4-methylbenzaldehyde, aniline and methyl acetoacetate for 20 min, at r.t. under

Table 3 Comparison of different catalysts for synthesis of piperidines

Entry	Catalyst	Solvent/condition	Reaction time	% Yield	Ref.
1	Sta-SO_3H (0.035 g)	None/rt	20 min	71	
2	$ZrOCl_2{\cdot}H_2O$ (20 mol%)	EtOH/Reflux	4 h	82	[39]
3	TBATB (10 mol%)	EtOH/rt	10 h	82	[19]
4	$Bi(NO_3)_3{\cdot}3H_2O$ (10 mol%)	EtOH/rt	18 h	76	[18]
5	$[K^+PEG]Br_3^-$ (10 mol%)	EtOH/rt	8 h	90	[41]
6	AcOH (5 mL)	None/rt	2 h	78	[44]
7	VCl_3 (10 mol%)	EtOH/rt	7 h	75	[42]
8	I_2 (10 mol%)	MeOH/rt	6 h	85	[16]
9	BDMS (10 mol%)	CH_3CN/rt	6 h	76	[17]
10	Tartaric acid (0.075 g)	MeOH/rt	7 h	87	[20]

[a] Reaction conditions: 4-chloro benzaldehyde (1 mmol), aniline (1 mmol), methyl acetoacetate (1 mmol)

[b] Isolated yields

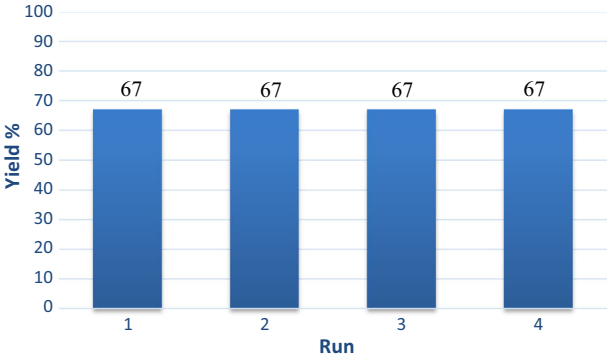

Fig. 4 The reuse of the catalyst

solvent-free conditions, and the results are displayed in Fig. 3. The separated catalyst can be reused after washing with ethyl acetate and drying at 100 °C. The catalyst was recovered in good yields and catalyst was used in the mentioned reaction for four successive reactions without significant loss of activity (Fig. 4).

Acylals are a useful carbonyl-protecting group because of their stability under both neutral and basic media and under acidic conditions [63]. Generally, acylals have been prepared by the reaction of aldehydes with acetic anhydride catalyzed by several reagents or catalysts such as $Bi(NO_3)_3{\cdot}5H_2O$ [64], silica-bonded S-sulfonic acid [65], saccharin sulfonic acid [66], cyanuric chloride [67], silica phosphoric acid [68], and $SiO_2/B(SO_4H)_3$ [69]. However, in these, some reported methods suffer from one or more drawbacks such as prolonged reaction times, use of environmentally unfavorable solvents and frequently low yields. Thus, the development of a new method for the synthesis of acylal derivatives would be highly desirable.

In order to check the catalytic activity of Sta-SO_3H as a solid acid, the synthesis of acylals was investigated. The optimum conditions for the acylation of benzaldehyde was achieved by treatment of benzaldehyde (1 mmol) with acetic anhydride (3 mmol) in the presence of Sta-SO_3H at r.t. under solvent-free conditions (Scheme 4). By following this reaction procedure, benzaldehyde derivatives were converted to the corresponding acylal in high yields. The results are summarized in Table 4.

Thermochemistry of reactions and spectroscopic analysis of products

Figure 3 shows the optimized geometry of the MPPC at M06-2X/6-311G(*d*,*p*) level of theory. This structure is minimal on the potential energy surface since there is no imaginary frequency. In this compound; the –NH of aniline fragment orients to the side of –C=O group of methyl acetoacetate part to make favored intramolecular hydrogen bonding (1.840 Å). Other important structural parameters of MPPC are indicated in Fig. 5.

Figure 6 shows the electrostatic potential (ESP) map and the electron density of highest and lowest molecular orbitals (HOMO and LUMO) for MPPC calculated by the M06-2X/6-311G(*d*,*p*) method. The red and blue positions in the ESP map

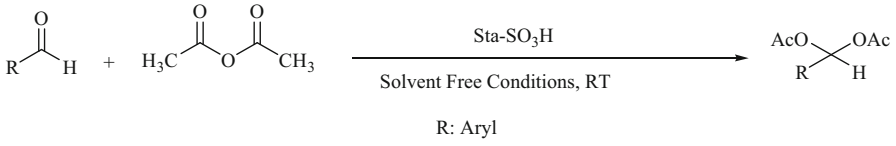

Scheme 4 Synthesis of acylals

Table 4 Conversion of aldehydes to the corresponding 1,1-diacetates by Sta-SO_3H as catalyst at r.t. and under solvent-free conditions

Entry	Substrate	Product[a]	Time (min)	Yield[b] (%)	m.p. °C [Ref.]	
					Found	Reported
1		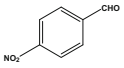	5	92	41–44	44–45 [70]
2	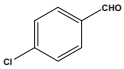	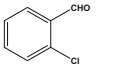	7	94	123–126	125–127 [70]
3		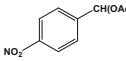	8	91	81–83	82–83 [70]
4	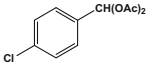	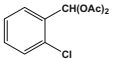	6	87	57–60	59 [71]

[a] The products were characterized from their spectral (IR and ^{1}H-NMR) and comparison to authentic samples

[b] The yields refer to the isolated pure products

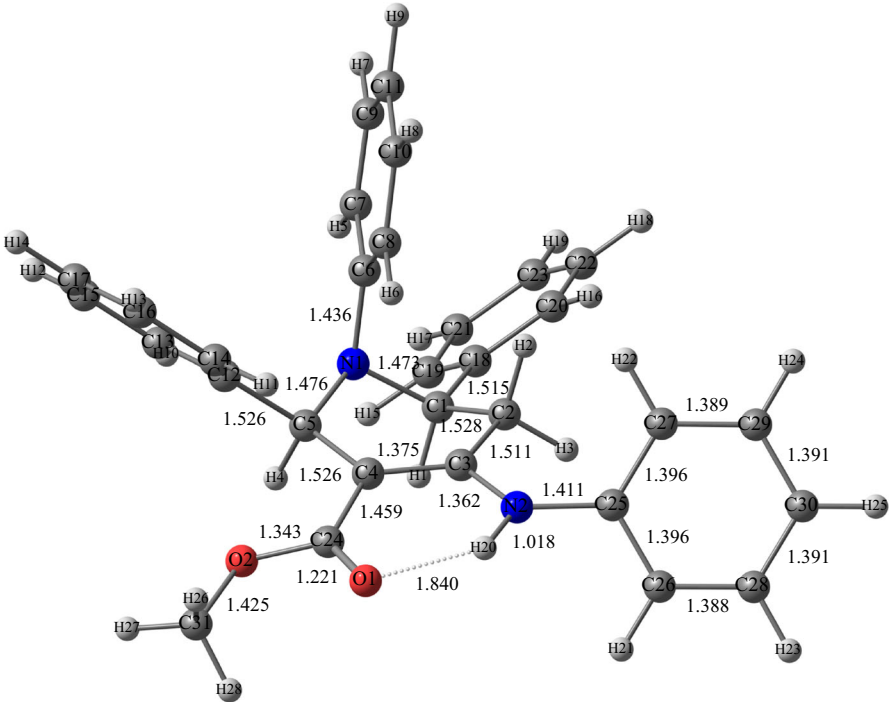

Fig. 5 The optimized structure of MPPC by M06-2X/6-311G(*d*,*p*) level of theory

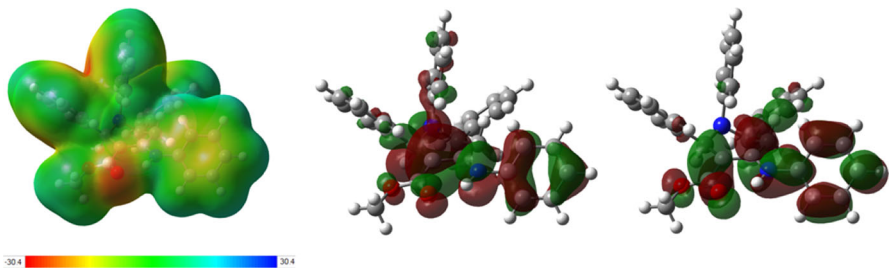

Fig. 6 ESP, HOMO and LUMO electron density maps for MPPC calculated by the M06-2X/6-311G(*d*,*p*) method (from *left* to *right*)

indicate the most negative and the most positive electrostatic potentials, respectively (unit for the legend is in kcal/mol). The calculated orbital energies of HOMO and LUMO and the energy separation between them which so calls ΔE_{gap} are −6.9, −0.1, 7.0 eV, respectively. As seen in this figure that the electron density of HOMO and LUMO are mostly delocalized on the piperidine ring and the aniline component of MPPC.

Table 5 lists the calculated thermochemical properties for the synthesis of MPPC using the multicomponent reaction of benzaldehyde, aniline and methyl

Table 5 Thermodynamic properties for synthesis of MPPC using the multicomponent reaction of benzaldehyde, aniline and methyl acetoacetate calculated at M06-2X/6-311G(*d*,*p*) level of theory

Property	
$\Delta_r U°$	−14.6
$\Delta_r H°$	−15.2
$\Delta_r S°$	−0.02
$\Delta_r G°$	−8.4

Energies are in kcal/mol and entropy is in kcal/mol K

acetoacetate (Scheme 1) at M06-2X/6-311G(*d*,*p*) level of theory. As the synthesis of highly functionalized piperidines in this work was performed at room temperature, gas phase enthalpy, internal energy, entropy and Gibbs free energy of reactions were calculated at 298.15 K. According to the results, all the thermodynamic properties of the multicomponent reaction at this temperature are negative. Formation of MPPC is an exothermic process ($\Delta_r H° = -15.2$ kcal/mol) accompanied by a decrease in internal energy ($\Delta_r U° = -14.6$ kcal/mol), entropy ($\Delta_r S° = -0.02$ kcal/mol K) and Gibbs free energy of reaction ($\Delta_r G° = -8.4$ kcal/mol). The negative value of the change in Gibbs free energy during the reaction indicates that the reaction can occur spontaneously under ambient temperature. As the number of product molecules is less than the number of molecules of the starting materials, the entropy of the reaction is also negative.

All the highly functionalized piperidines listed in Table 2 were known compounds and characterized by IR, ^{1}H NMR, and ^{13}C NMR spectra and well matched with the literature-reported compounds. In the following, these results for one of the general compound entry 5 are discussed. A broad range of IR spectrum of this compound (400–3600) cm^{-1}, is covered by bending and stretching vibrations (Fig. 7, top). The peaks observed around 3200 cm^{-1} corresponds to the N–H stretching mode. The wide peaks around 3000–3100 cm^{-1} are assigned to the stretching sp^2 = C–H vibrations. The peaks appearing below 3000 cm^{-1} are related to the sp^3 –C–H stretching modes. The sharp peak observed at 1660 cm^{-1} is attributed to the C=O stretching mode, which is shifted to lower frequencies than the normal position of the C=O group in esters, i.e. 1730–1750 cm^{-1} (because conjugation with C=C and intramolecular hydrogen bonding to N–H). The C=C stretch adsorptions are seen at 1618, 1596 and 1498 cm^{-1}. The peak around 1200 cm^{-1} is related to the C–O stretching mode. Using the scaling factor of 0.94 for the calculated data at M06-2X/6-311G(*d*,*p*) level of theory, a good consistency between the calculated and observed spectra was found. For example the N–H, C=O, C=C and C–O stretching modes appear at 3256, 1654, (1575, 1554, 1401) and 1238 cm^{-1},respectively (Fig. 7, bottom).

Table 6 lists the calculated ^{1}H NMR chemical shifts (δ, ppm) for MPPC in the gas phase and in chloroform as solvent via B3LYP/6-311 + G(2*d*,*p*) level of theory (vs. TMS) (see also Fig. 8). The experimental spectrum recorded in $CDCl_3$ is shown in Fig. 8. Due to intramolecular NH···O hydrogen bonding, the hydrogen atom

Table 6 ^{1}H NMR chemical shifts (δ, ppm) for MPPC calculated via B3LYP/6-311 + G(2*d*,*p*) level of theory in comparison to experimental data

H atoms	Calculated		Experimental	
	Gas phase	In solvent	In solvent	Explanation
–NH (H20)	11.2	11.2	10.3	Singlet, 1H
Phenyl rings (H5–H19, H21–25)	6–8.2	6–8.2	6.4–7.3	Multiplet, 20H
–CH (H4)	6.3	6.3	6.4	Singlet, 1H
–CH (H1)	4.8	4.8	5.1	doublet, 1H
$–CH_2$ (H2, H3)	2.4, 3.4	2.4, 3.4	2.8, 2.9	Doublet of doublet, 2H
$–OCH_3$ (H26–H28)	3.7	3.7	3.9	Singlet, 3H

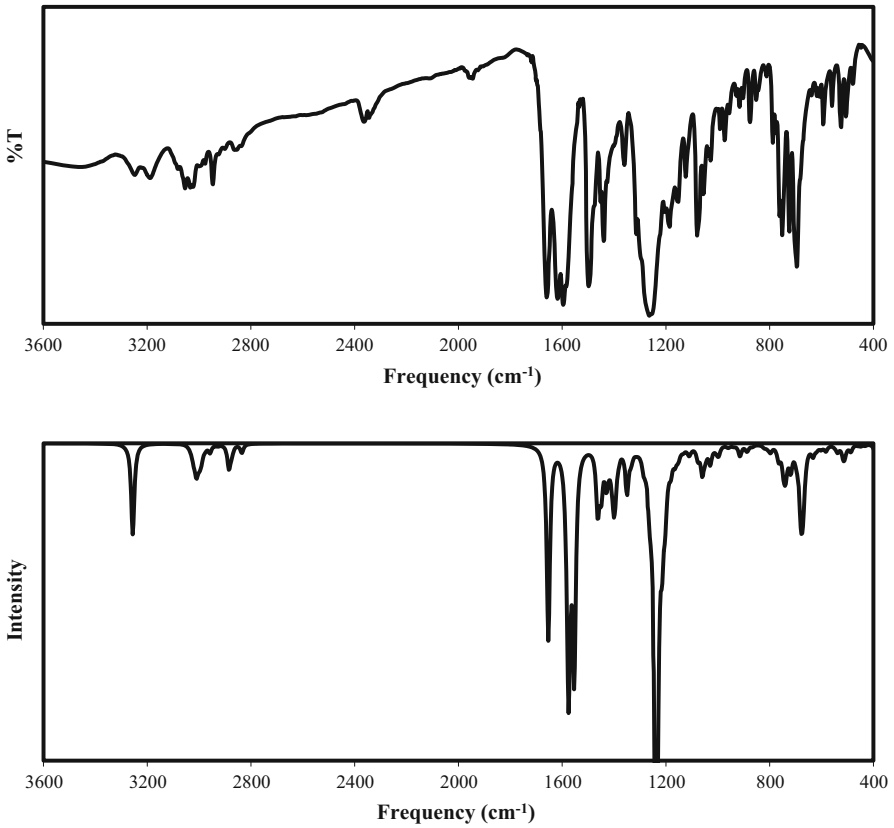

Fig. 7 Experimental FTIR spectrum of MPPC (*top*) in comparison to the calculated data using M06-2X/6-311G(*d*,*p*) level of theory with scaling factor of 0.94 (*bottom*)

attached to nitrogen (H20) markedly shifts downfield and appears close to 10.3 ppm. The hydrogen atoms attached to aromatic rings are seen at 6.4–7.3 ppm. The single peaks at 5.1 and 6.4 are related to benzylic-allylic –CH (H4) and

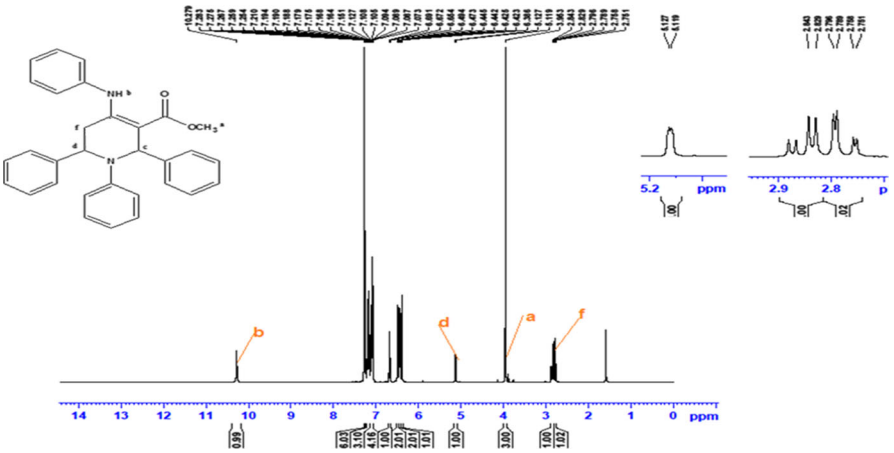

Fig. 8 ^{1}H NMR spectrum of MPPC recorded in $CDCl_3$ as solvent

benzylic –CH (H1), respectively. The hydrogen atoms of $–CH_2$ (H2, H3) are diasterotopic and appear in the area of 2.8 and 2.9 as a doublet of doublet. The hydrogen atoms of $OCH_3$are singlet and they resonance at 3.9 ppm. An acceptable agreement was found between the calculated and observed spectroscopic data (Table 6).

Conclusion

A novel carbon-based solid acid has been synthesized through the simple heat treatment of sulfuric acid and starch. The novel process was more environmentally friendly in the mild condition with little waste emissions and high yield. Here, we have found that the formation of highly functionalized piperidines is possible in the presence of Sta-SO_3H as catalyst via a one-pot five-component reaction at room temperature from readily available starting materials. Some advantages of this MCRs protocol are good yields, mild reaction conditions, environmentally benign catalyst, absence of tedious separation procedures, superior atom economy, and low cost. The catalyst has the advantages of high acidity, low cost and high thermal and chemical stability, which made the novel heterogeneous catalyst have great potential for the replacement of the homogeneous catalysts in the green process. Density functional theory (DFT) calculations were used to study the structure of MPPC as well as the thermochemistry of the multicomponent reaction. The theoretically calculated infrared (IR) and ^{1}H nuclear magnetic resonance (NMR) spectra were compared to the experimental data. It was found that the synthesis of highly functionalized piperidines is exothermic accompanied by a decrease in entropy, internal energy and Gibbs free energy of reaction. Also, good consistency between the calculated and observed spectral data was found. On the other hand, an efficient and rapid catalytic method was achieved for the preparation of acylals

using this catalyst at room temperature and under solvent-free conditions. The mild condition, eco-friendliness, good to high yields, short reaction times and use of an inexpensive and reusable catalyst are important features of this method.

References

1. B. Zhang, J. Ren, X. Liu, Y. Guo, Y. Guo, G. Lu, Y. Wang, Catal. Commun. **11**, 629–632 (2010)
2. Y. Lu, X. Liang, C. Qi, Bull. Mater. Sci. **35**, 419–424 (2012)
3. X. Wang, R. Liu, M.M. Waje, Z. Chen, Y. Yan, K.N. Bozhilov, P. Feng, Chem. Mater. **19**, 2395–2397 (2007)
4. R. Liu, X. Wang, X. Zhao, P. Feng, Carbon **46**, 1664–1669 (2008)
5. J. Janaun, N. Ellis, Appl. Catal. A **394**, 25–31 (2011)
6. B. Chang, J. Fu, Y. Tian, X. Dong, J. Phys. Chem. C **117**, 6252 (2013)
7. B. Chang, Y. Tian, W. Shi, J. Liu, F. Xi, X. Dong, RSC Adv. **3**, 20999–21006 (2013)
8. B. Chang, J. Fu, Y. Tian, X. Dong, RSC Adv. **3**, 1987–1994 (2013)
9. X. Liu, M. Huang, H.L. Ma, Z.Q. Zhang, J.M. Gao, Y.L. Zhu, X.J. Han, X.Y. Guo, Molecules **15**, 7188–7196 (2010)
10. Y. Zhao, H. Wang, Y. Zhao, J. Shen, Catal. Commun. **11**, 824–828 (2010)
11. L. Xuezheng, L. Chunqing, Q. Chenze, J. Mater. Sci. **46**, 5345–5349 (2011)
12. S. Brauch, S.S. Van Berkel, B. Westermann, Chem. Soc. Rev. **42**, 4948–4962 (2013)
13. T.J.J. Müller, Science of Synthesis, Multicomponent Reactions I (Georg Thieme Verlag KG, Stuttgart, 2014)
14. C. Hulme, M. Ayaz, G. Martinez-Ariza, F. Medda, A. Shaw, Small Molecule Medicinal Chemistry: Strategies and Technologies, ed. W. Czechtizky, P. Hamley, Wiley, Weinheim, ch. 6, 145–187 (2015)
15. C. Hulme, V. Gore, Curr. Med. Chem. **10**(1), 51–80 (2003)
16. A.T. Khan, M.M. Khan, K.K.R. Bannuru, Tetrahedron **66**, 7762–7772 (2010)
17. A.T. Khan, T. Parvin, L.H. Choudhury, J. Org. Chem. **73**, 8398–8402 (2008)
18. G. Brahamachari, S. Das, Tetrahedron Lett. **53**, 1479–1484 (2012)
19. A.T. Khan, M. Lal, M.M. Khan, Tetrahedron Lett. **51**, 4419–4424 (2010)
20. J. Aboonajmi, M.T. Maghsoodlou, N. Hazeri, M. Lashkari, M. Kangani, Res. Chem. Intermed. **41**, 8057–8065 (2015)
21. D. Elbein, R. Molyneux, in S.W. Pelletier, Ed. Alkaloids, chemical and biological perspectives (Wiley, New York, 1987), p. 57
22. D. O'Hagan, Nat. Prod. Rep. **17**, 435–446 (2000)
23. J.W. Daly, T.F. Spande, H.M. Garraffo, J. Nat. Prod. **68**, 1556–1575 (2005)
24. J. Esquivias, R.G. Arrayas, J.C. Carretero, J. Am. Chem. Soc. **129**, 1480–1481 (2007)
25. X.-F. Zhu, J. Lan, O. Kwon, J. Am. Chem. Soc. **125**, 4716–4717 (2003)
26. J.F.H. Takemiya, J. Am. Chem. Soc. **128**, 6042–6043 (2006)
27. R. Martín, C. Murruzzu, M.A. Pericàs, A. Riera, J. Org. Chem. **70**, 2325–2328 (2005)
28. T.P. Lebold, A.B. Leduc, M.A. Kerr, Org. Lett. **11**, 3770–3772 (2009)
29. K. Takasu, N. Shindoh, H. Tokuyama, M. Ihara, Tetrahedron **62**, 11900–11907 (2006)
30. M. Sales, A.B. Charette, Org. Lett. **7**, 5773–5776 (2005)
31. M.S.R. Murty, R. Ram, J.S. Yadav, Tetrahedron Lett. **49**, 1141–1145 (2008)
32. R.M. Carballo, M.A. Ramirez, M.L. Rodriguez, V.S. Martin, J.I. Padron, Org. Lett. **8**, 3837–3840 (2006)
33. A.P. Dobbs, S.J. Guesne, J. Synlett. 2101–2104 (2005)
34. S. Fustero, D. Jimenez, J. Moscardo, S. Catalan, C. del Pozo, Org. Lett. **9**, 5283–5286 (2007)
35. F.A. Davis, B. Chao, A. Rao, Org. Lett. **3**, 3169–3171 (2001)
36. P.A. Clarke, A.V. Saytsev, A.C. Whitwood, Tetrahedron Lett. **48**, 5209–5212 (2007)
37. M. Misra, S.K. Pandey, V.P. Pandey, J. Pandey, R. Tripathi, R.P. Tripathi, Bioorg. Med. Chem. **17**, 625 (2009)
38. H.-J. Wang, L.-P. Mo, Z.-H. Zhang, ACS. Comb. Sci. **13**, 181 (2011)
39. S. Mishra, R. Ghosh, Tetrahedron Lett. **52**, 2857 (2011)

40. C. Mukhopadhyay, S. Rana, R.J. Butcher, A.M. Schmiedekamp, Tetrahedron Lett. **52**, 5835–5840 (2011)
41. S. Verma, S.L. Jain, B. Sain, Beilstein J. Org. Chem. **7**, 1334–1341 (2011)
42. S. Pal, L.H. Choudhury, T. Parvin, Mol. Divers. **16**, 129 (2012)
43. R. Ramachandran, S. Jayanthi, Y.T. Jeong, Tetrahedron **68**, 363–369 (2012)
44. M. Lashkari, M.T. Maghsoodlou, N. Hazeri, S.M. Habibi-Khorassani, S.S. Sajadikhah, R. Doostmohamadi, Synth. Commun. **43**, 635–644 (2013)
45. H. Eshghi, A. Khojastehnezhad, F. Moeinpour, S. Rezaeian, M. Bakavoli, M. Teymouri, A. Rostami, K. Haghbeen, Tetrahedron **71**, 436–444 (2015)
46. W.M. Basyouni, K.A.M. El-Bayouki, W.M. Tohamy, S.Y. Abbas, Synth. Commun. **45**, 1073–1081 (2015)
47. Y. Zhao, D.G. Truhlar, Theor. Chem. Acc. **120**, 215–241 (2008)
48. F. London, J. Phys. Radium. **8**, 397–409 (1937)
49. R. Ditchfield, Mol. Phys. **27**, 789–807 (1974)
50. M.J. Frisch, G.W. Trucks, H.B. Schlegel, G.E. Scuseria, M.A. Robb, J.R. Cheeseman, J.A. Montgomery, Jr., T. Vreven, K.N. Kudin, J.C. Burant, J.M. Millam, S.S. Iyengar, J. Tomasi, V. Barone, B. Mennucci, M. Cossi, G. Scalmani, N. Rega, G.A. Petersson, H. Nakatsuji, M. Hada, M. Ehara, K. Toyota, R. Fukuda, J. Hasegawa, M. Ishida, T. Nakajima, Y. Honda, O. Kitao, H. Nakai, M. Klene, X. Li, J.E. Knox, H.P. Hratchian, J.B. Cross, V. Bakken, C. Adamo, J. Jaramillo, R. Gomperts, R.E. Stratmann, O. Yazyev, A.J. Austin, R. Cammi, C. Pomelli, J.W. Ochterski, P.Y. Ayala, K. Morokuma, G.A. Voth, P. Salvador, J.J. Dannenberg, V.G. Zakrzewski, S. Dapprich, A.D. Daniels, M.C. Strain, O. Farkas, D.K. Malick, A.D. Rabuck, K. Raghavachari, J.B. Foresman, J.V. Ortiz, Q. Cui, A.G. Baboul, S. Clifford, J. Cioslowski, B.B. Stefanov, G. Liu, A. Liashenko, P. Piskorz, I. Komaromi, R.L. Martin, D.J. Fox, T. Keith, M.A. Al-Laham, C.Y. Peng, A. Nanayakkara, M. Challacombe, P.M.W. Gill, B. Johnson, W. Chen, M.W. Wong, C. Gonzalez, J. A. Pople, Gaussian 09, Revision B.01 (Gaussian, Inc., Wallingford, CT, 2009)
51. M.H. Zong, Z.Q. Duan, W.Y. Lou, T.J. Smith, H. Wu, Green Chem. **9**, 434–437 (2007)
52. Q. Shu, J. Gao, Z. Nawaz, Y. Liao, D. Wang, J. Wang, Appl. Energy **87**, 2589–2596 (2010)
53. K. Nakajima, M. Hara, ACS Catal. **2**, 1296–1304 (2012)
54. V. Mirkhani, M. Moghadam, S. Tangestaninejad, I. Mohammadpoor-Baltork, M. Mahdavi, Monatsh. Chem. **140**, 1489–1494 (2009)
55. S.A. Pourmousavi, H. Salahshornia, Bull. Korean Chem. Soc. **32**, 1575 (2011)
56. S.A. Pourmousavi, ShS Kazemi, Monatsh. Chem. **143**, 917–923 (2011)
57. F. Fahid, S.A. Pourmousavi, J. Sulfur Chem. **36**, 16–29 (2014)
58. S.A. Pourmousavi, A. Kanaani, F. Ghorbani, K.K. Damghani, D. Ajloo, M. Vakili, Res. Chem. Intermed. doi:10.1007/s11164-015-2084-4
59. P.A. Clarke, A.V. Zaytzev, A.C. Whitwood, Tetrahedron Lett. **48**, 5209–5212 (2007)
60. P.A. Clarke, A.V. Zaytzev, A.C. Whitwood, Synthesis **2008**, 3530–3532 (2008)
61. S.S. Sajadikhah, M.T. Maghsoodlou, N. Hazeri, S.M. Habibi-Khorassani, A.C. Willis, Chin. Chem. Lett. **23**, 569–572 (2012)
62. S. Mishra, R. Ghosh, Tetrahedron Lett. **52**, 2857–2861 (2011)
63. K.S. Kochhar, B.S. Bal, R.P. Deshpande, S.N. Rajadhyaksha, H.W. Pinnick, J. Org. Chem. **48**, 1765–1767 (1983)
64. D.H. Aggen, J.N. Arnold, P.D. Hayes, N.J. Smoter, R.S. Mohan, Tetrahedron **60**, 3675–3679 (2004)
65. Kh Niknam, D. Saberi, M.N. Sefat, Tetrahedron Lett. **50**, 4058–4062 (2009)
66. F. Shirini, M. Mamaghani, M. Abedini, Bull. Korean Chem. Soc. **31**, 2399–2401 (2010)
67. B.P. Bandgar, N.S. Joshi, V.T. Kamble, J. Chin. Chem. Soc. **54**, 489–492 (2007)
68. F. Zhang, H. Liu, Q.J. Zhang, Y.Z. Zhao, F.L. Yang, Synth. Commun. **40**, 3240–3250 (2010)
69. S. Sajjadifar, S. Rezayati, Chem. Pap. **68**, 531–539 (2014)
70. T.S. Jin, G. Sun, Y.W. Li, T.S. Li, Green Chem. **4**, 255–256 (2002)
71. B.R. Jermy, A. Pandurangan, Catal. Commun. **9**, 577–583 (2008)